Intricate Interaction Between Store-Operated Calcium Entry and Calcium-Activated Chloride Channels in Pulmonary Artery Smooth Muscle Cells

Abigail S. Forrest, Jeff E. Angermann, Rajesh Raghunathan, Catherine Lachendro, Iain A. Greenwood, and Normand Leblanc

Abstract Ca^{2+}-activated Cl^- channels (Cl_{Ca}) represent an important excitatory mechanism in vascular smooth muscle cells. Active accumulation of Cl^- by several classes of anion transporters results in an equilibrium potential for this ion about 30 mV more positive than the resting potential. Stimulation of Cl_{Ca} channels leads to membrane depolarization, which enhances Ca^{2+} entry through voltage-gated Ca^{2+} channels and leads to vasoconstriction. Cl_{Ca} channels can be activated by distinct sources of Ca^{2+} that include (1) mobilization from intracellular Ca^{2+} stores (ryanodine or inositol 1,4,5-trisphosphate [$InsP_3$]) and (2) Ca^{2+} entry through voltage-gated Ca^{2+} channels or reverse-mode Na^+/Ca^{2+} exchange. The present study was undertaken to determine whether Ca^{2+} influx triggered by store depletion (store-operated calcium entry, SOCE) activates Cl_{Ca} channels in rabbit pulmonary artery (PA) smooth muscle. Classical store depletion protocols involving block of sarcoplasmic reticular Ca^{2+} reuptake with thapsigargin (TG; 1 μM) or cyclopiazonic acid (CPA; 30 μM) led to a consistent nifedipine-insensitive contraction of intact PA rings and rise in intracellular Ca^{2+} concentration in single PA myocytes that required the presence of extracellular Ca^{2+}. In patch clamp experiments, TG or CPA activated a time-independent nonselective cation current (I_{SOC}) that (1) reversed between –10 and 0 mV; (2) displayed the typical "N"-shaped current–voltage relationship; and (3) was sensitive to the (I_{SOC}) blocker by SKF-96365 (50 μM). In double-pulse protocol experiments, the amplitude of I_{SOC} was varied by altering membrane potential during an initial step that was followed by a second constant step to +90 mV to register Ca^{2+}-activated Cl^- current, $I_{Cl(Ca)}$. The niflumic acid-sensitive time-dependent

A.S. Forrest, R. Raghunathan, C. Lachendro, and N. Leblanc (✉)
Department of Pharmacology, Center of Biomedical Research Excellence (COBRE), University of Nevada School of Medicine, 1664 North Virginia, Reno, NV, 89557-0270, USA
e-mail: NLeblanc@Medicine.Nevada.edu

J.E. Angermann
Department of Environmental and Occupational Health, School of Community Health Sciences, University of Nevada, Reno, NV, USA

I.A. Greenwood
Division of Basic Medical Sciences, St George's, University of London, London, UK

J.X.-J. Yuan and J.P.T. Ward (eds.), *Membrane Receptors, Channels and Transporters in Pulmonary Circulation*, AEME, Vol. 661, DOI 10.1007/978-1-60761-500-2_3,

$I_{Cl(Ca)}$ at +90 mV increased in proportion to the magnitude of the preceding hyperpolarizing step, an effect attributed to graded membrane potential-dependent Ca^{2+} entry through I_{SOC} and confirmed in dual patch clamp and Fluo-5 experiments to record membrane current and free intracellular Ca^{2+} concentration simultaneously. Reverse-transcription polymerase chain reaction (RT-PCR) experiments confirmed the expression of several molecular determinants of SOCE, including transient receptor potential canonical (TRPC) 1, TRPC4, and TRPC6; stromal interacting molecule (STIM) 1 and 2; and Orai1 and 2, as well as the novel and probable molecular candidates thought to encode for Cl_{Ca} channels transmembrane protein 16A (TMEM16A) Anoctamin 1 (ANO1) and B (ANO2). Our preliminary investigation provides new evidence for a Ca^{2+} entry pathway consistent with store-operated Ca^{2+} entry signaling that can activate Ca^{2+}-activated Cl^- channels in rabbit PA myocytes. We hypothesize that this mechanism may be important in the regulation of membrane potential, Ca^{2+} influx, and tone in these cells under physiological and pathophysiological conditions.

Keywords Calcium-activated chloride channels • store-operated calcium entry (SOCE) • capacitative calcium entry (CCE) • vascular smooth muscle cells pulmonary arterial tone • contraction • intracellular calcium concentration • whole-cell patch clamp technique • TMEM16a • STIM1 • Orai • TRPC

1 Introduction

In many nonexcitable and excitable cell types, depletion of endoplasmic reticulum (ER) Ca^{2+} stores triggers the opening of channels in the plasma membrane that enable store replenishment. Physiologically, this process is activated by an agonist binding to a surface receptor, generally a G protein-coupled receptor (e.g., G_q) that triggers the synthesis of the second messenger diacylglycerol (DAG) and inositol 1,4,5-trisphosphate (IP_3) originating from the breakdown of the membrane phospholipid phosphatidylinositol. Whereas DAG serves as an activator of protein kinase C, an important signaling kinase, IP_3 binds to a Ca^{2+} channel receptor in the ER ($InsP_3$ or $InsP_3R$) that promotes Ca^{2+} mobilization, yielding a cellular response (e.g., contraction, secretion of a hormone or neurotransmitter, etc.).[1] The plasma membrane Ca^{2+} influx pathway stimulated by IP_3-mediated emptying of the Ca^{2+} stores or capacitative calcium entry (CCE), was originally proposed by Putney[2] and is now routinely referred to as store-operated calcium entry (SOCE). SOCE has been reported in a number of vascular smooth muscle cells, including pulmonary artery (PA) myocytes.[3–6]

The nature of the ionic conductance at the plasma membrane and mechanism by which SOCE mediates its activation is far from being understood but has received a lot of attention in light of the discovery of new molecular candidates participating in this pathway. Patch clamp studies revealed two different types of ionic current behaviors evoked by SOCE in different cell types: (1) a current mediated by a Ca^{2+} release-activated channel called I_{CRAC} (or CRAC) displaying high selectivity for Ca^{2+}

was first described in T lymphocytes and the commonly used Jurkat cell model[7]; (2) a nonselective cation channel (NSCC) current.[4,8,9] I_{CRAC} was the first SOCE-induced ionic current described. The underlying Ca^{2+}-selective channel displays strong inward rectification and a single-channel conductance that is below the resolution of the patch clamp technique and could only be indirectly inferred from fluctuation analysis of stationary and nonstationary analysis of I_{CRAC}. The NSCC current (I_{NSCC}) elicited by store depletion exhibits variable rectifying properties and a reversal potential lying between ~ –10 and +10 mV. The channels are mostly permeable to monovalent cations such as Na^+ and K^+ but exhibit significant permeability to Ca^{2+}. The single-channel conductance is also higher than that of CRAC channels. Relatively recent reports have provided evidence that homo- or heterotetrameric channels formed by one or several members of the canonical transient receptor potential (TRPC) family of genes may be an integral part of the pore-forming subunit of the NSCC activated by store depletion (TRPC1, TRPC4, TRPC5, and in some cases TRPC6).[9] Wide genomic screening techniques identified two new gene families, Orai and the stromal interacting molecule (STIM), which were suggested to form the molecular basis of I_{CRAC}.[10] Studies have shown that Orai proteins (Orai1–3) are transmembrane proteins found in a wide variety of cell types[11], and it has been suggested that Orai1 may be the pore-forming subunit of the I_{CRAC} channel.[12] In addition, overexpression studies also indicated that Orai2 is likely involved in the formation of I_{CRAC} channels as it also produces augmented currents but with lower efficacy than Orai1.[13] It seems doubtful that Orai3 is at all responsible for this current.[13] STIM1 and STIM2 are transmembrane proteins located in the ER and plasma membrane and speculated to act as the sensor for ER Ca^{2+} depletion, although the exact role of STIM2 in SOCE will require further investigation. Following store depletion, STIM1 would somehow aggregate near the plasma membrane and trigger the opening of Orai1 via a protein–protein interaction.[14] Evidence has also linked the activation of TRPC1 (and thus I_{NSCC}) to STIM1 through a dynamic trafficking process involving lipid rafts.[15] It has also been suggested that Orai1, TRPC1, and STIM1 may form a structural and dynamic trio of proteins allowing for a flexible array of SOCE patterns in the same cell.[16–18]

Since 2001, our group has focused on the elucidation of the biophysical properties, pharmacology, regulation, and functional significance of Ca^{2+}– activated Cl^- channels (Cl_{Ca}) in arterial and venous smooth muscle cells. These channels are believed to be important in signal transduction because their activation causes membrane depolarization.[19,20] This is due to an equilibrium potential for Cl^- that is about 20–30 mV more positive than the resting membrane potential of vascular smooth muscle cells and is the product of active accumulation of Cl^- by ion transporters. These channels are activated by a rise in intracellular Ca^{2+} concentration above about 180 n*M* and are modulated by voltage. Cl_{Ca} channels can be activated by distinct sources of Ca^{2+}, which include Ca^{2+} entry through voltage-gated Ca^{2+} channels or reverse-mode Na^+/Ca^{2+} exchange, or from mobilization of intracellular Ca^{2+} stores that may occur spontaneously due to short-lived spontaneous Ca^{2+} release events from ryanodine receptors in the sarcoplasmic reticulum (SR) or Ca^{2+} sparks (so-called STICs, standing for spontaneous transient inward currents) or evoked by stimulation by an agonist leading to the production of IP_3 and subsequent Ca^{2+} release from the SR.

The very low conductance Cl_{Ca} channel (~1–3 pS) displays strong outward rectification, especially at low to moderate levels of $[Ca^{2+}]_i$, and typical slow activation and deactivation kinetics at positive and negative potentials, respectively. The CLCA, Tweety, Bestrophin, and very recently the TMEM16A/B gene families have been proposed as molecular candidates encoding for Cl_{Ca} channels.[21–23] The CLCA family is most likely not a bona fide ion channel and is now speculated to be a regulator of Cl^- conductance. Some members of the Tweety family encode for Ca^{2+}-activated Cl^- channels, but their conductance is very high (>250 pS) and therefore does not fit the profile of the very-low-conductance Cl_{Ca} channel identified in native cells. Several members of the Bestrophin family of genes form Cl^--permeable small conductance channels that are activated by relatively high-affinity binding of Ca^{2+} ($K_d \approx 250$ n*M*); however the channels are voltage insensitive and lack time dependence. Three independent groups presented evidence suggesting that expression of TMEM16A (and TMEM16B in one study) in various heterologous expression cell systems generates a membrane current that is consistent with native Ca^{2+}-activated Cl^- currents recorded in many secretory and retinal epithelia, smooth muscle, and sensory neurons.[24–26] Common properties include (1) an identical anion permeability sequence ($SCN^- >> NO_3^- > I^- > Br^- > Cl^- >> F^- >>$ gluconate); (2) a voltage-sensitive K_d for activation by intracellular Ca^{2+}, (3) a low single-channel conductance (8.3 pS); and (4) time- and voltage-dependent macroscopic currents exhibiting outward rectification, slow activation on depolarization, and slow deactivation following repolarization.

Several groups of investigators have previously demonstrated the existence of SOCE in smooth muscle from PAs[3,27] and may thus represent an additional Ca^{2+} entry pathway for activation of Cl_{Ca} channels. The purpose of the present study undertaken in rabbit PA smooth muscle cells was twofold: (1) to test the hypothesis that Ca^{2+} entry elicited by store depletion can stimulate Cl_{Ca} channels and (2) to carry out a preliminary investigation of the expression profile of molecular candidates suspected to be involved in generating SOCE and Cl_{Ca} channels.

2 Materials and Methods

2.1 Isolation of Pulmonary Artery Myocytes

A similar method to that previously used by our group[28,29] was used to isolate smooth muscle cells. In brief, cells were prepared from the main and secondary PA branches dissected from New Zealand white rabbits (2–3 kg) killed by anesthetic overdose in accordance with British and American guidelines for animal care. After dissection and removal of connective tissue, the PAs were cut into small strips and incubated overnight (~16 h) at 4°C in a low-Ca^{2+} physiological salt solution (PSS; see composition in Section 3.2.5) containing 10 μ*M* $CaCl_2$ and about 1 mg/mL papain, 0.15 mg/mL dithiothreitol, and 1 mg/mL bovine serum albumin.

The next morning, the tissue strips were rinsed three times in low-Ca^{2+} PSS and incubated in the same solution for 5 min at 37°C. Cells were released by gentle agitation with a wide-bore Pasteur pipet and then stored at 4°C until used (within 10 h following dispersion).

2.2 Contractile Studies

The main branch of rabbit PA was dissected, placed in cold PSS, and cleaned of connective and adipose tissue. The artery was then denuded of endothelium by bubbling a gentle stream of O_2 through the intact vessels and was then cut into rings of about 3–5 mm, which were immersed in well-oxygenated PSS (95% O_2, 5% CO_2) at 37°C and mounted for tension measurements in a 30-mL bathing chamber. One of the rings was fixed via tungsten triangular mounting wire to the bottom of the chamber; the other end was hung via a similar tungsten triangular wire connected to a Grass Technologies FT03 force transducer to measure isometric force. The output of the force transducer was connected to a WPI TBM 4 Transbridge amplifier, and the amplified signal was recorded via a MP100 BIOPAC Systems analog-to-digital converter controlled by Acknowledge Software (v. 3.5.3) running on a Windows Millennium-based Pentium II Dell personal computer (PC). Rings were allowed to equilibrate for 60 min in normal PSS at a resting tension of 0.5 g before being challenged with two exposures (20 and 5 min, respectively) to 85.4 m*M* KCl to verify their responsiveness.

2.3 Patch Clamp Electrophysiology and Experimental Protocols

The nystatin-perforated or standard whole-cell configuration of the patch clamp technique was used to record macroscopic currents from freshly isolated vascular smooth muscle cells. Perforated patch access was achieved through dialysis of 400 mg nystatin per milliliter internal solution, which developed over the course of 10 min following pipet-to-cell sealing as monitored from the acceleration of the capacitative current transients elicited by repetitive 5- to 10-mV steps (100 Hz) from a holding potential (HP) of –50 mV applied by the internal pulse generator of the patch clamp amplifier. Patch pipets were manufactured from borosilicate glass and then fire polished to produce pipets with resistances of about 2 MΩ when filled with the perforated patch internal solution described in Section 3.2.5. Bathing solutions were gravity perfused from a 50-mL syringe barrel at an approximate flow rate of 1 mL/min, resulting in a complete bath exchange time of ~1 min.

All currents were monitored with an Axopatch 1D or Axopatch 200A patch clamp amplifier (Axon CNS, Molecular Devices) at room temperature (20–23°C). Output signals were filtered at 1 kHz by the patch clamp amplifier and sampled at 10 kHz via a Digidata 1322A acquisition system and pCLAMP 9.0 software

(Axon CNS, Molecular Devices) run on a Pentium IV Dell PC under Windows XP. L-type Ca^{2+} currents were elicited by stepping membrane potential to +20 mV every 20 s from an HP of –70 mV. Store-operated cation and Ca^{2+}-activated Cl^- currents induced by the store-depleting agent thapsigargin (TG) or cyclopiazonic acid (CPA) were recorded from an HP of 0 mV that consisted of a double-pulse protocol by which membrane potential was initially stepped for 1–2 s from one or a series of steps ranging from –100 to +60 mV. This initial step was used to measure the nonselective cation current in isolation and to alter the driving force for Ca^{2+} entry. A second step lasting 1–5 s to +90 or +130 mV served to elicit time-dependent Ca^{2+}-activated Cl^- current $I_{Cl(Ca)}$ and examine the impact of the preceding conditioning voltage step on the magnitude of $I_{Cl(Ca)}$. In some experiments, the second step was followed by a repolarizing step (500 ms) to –80 mV to record $I_{Cl(Ca)}$ tail.

2.4 Intracellular Ca^{2+} Concentration Measurements

Free intracellular Ca^{2+} concentration was measured with the Ca^{2+} indicator Fluo-4 or Fluo-5F. For the experiments described in Fig. 3.1c, cells were preincubated with 5 μ*M* of the ester form of the indicator (Fluo-4 AM) for 45 min at room temperature. Experiments were initiated after at least 30 min of washout of the indicator to allow for complete intracellular deesterification of the dye. These experiments were carried out using an ×40 Fluor Nikon objective (numerical aperture [NA] = 1.3) housed on an inverted Nikon Diaphot 300 microscope. Fluo-4 or Fluo-5F was excited at 490 nm with a 75-W xenon arc lamp, and epifluorescent light from the entire cell (restrained by a mechanical diaphragm) was measured at 520 nm. Epifluorescent light collected through the lateral port of the microscope was transmitted to a highly sensitive Hamamatsu photomultiplier tube housed in the spectral separator of a Solamere Technology Group SFX-2 Ratiometric Fluorometer system. The emitted Fluo-4 or Fluo-5F fluorescence signal at 520 nm was expressed relative to basal fluorescence recorded in the presence of nifedipine (F/F_0) and digitized via a Digidata 1322A acquisition system and pCLAMP 9.0 software (Axoscope or Clampex, Axon CNS, Molecular Devices) run on a Pentium IV Dell PC under Windows XP.

2.5 Solutions and Reagents

The composition of the normal PSS used in contractility experiments (Fig. 4.1a, b) was as follows (in m*M*): NaCl (120), KCl (4.2), $NaHCO_3$ (25; pH 7.4 after equilibration with 95% O_2/5% CO_2 gas), KH_2PO_4 (1.2), $MgCl_2$ (1.2), glucose (11), and $CaCl_2$ (1.8). All rings were challenged with a high-KCl solution made by substituting 80 m*M* NaCl of the above solution with 80 m*M* KCl. Single PA smooth muscle cells were isolated by incubating PA tissue strips in the following low-Ca^{2+} (10 μ*M*)

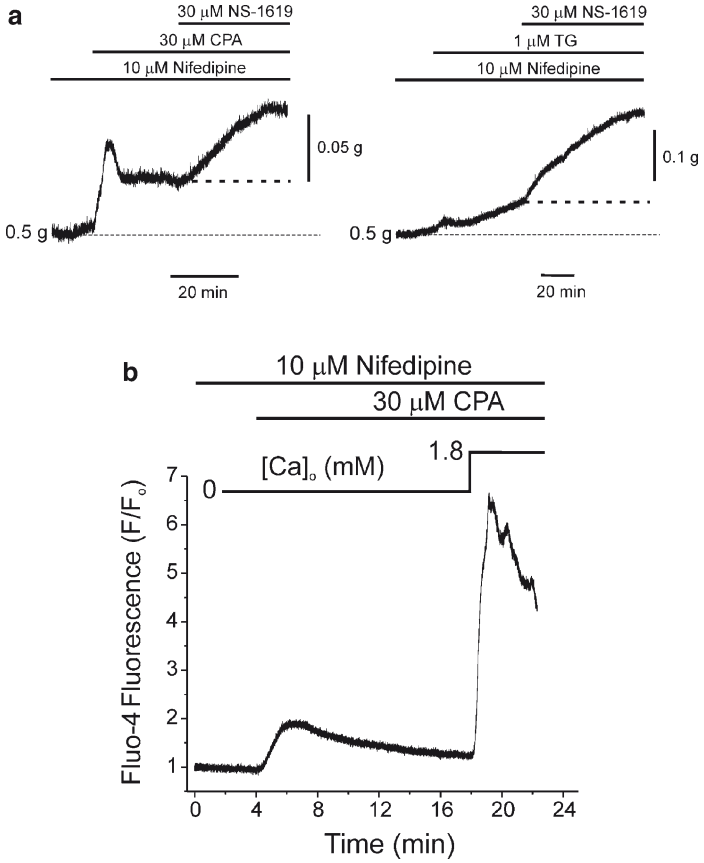

Fig. 3.1 Store depletion elicits contraction and Ca^{2+} transient in rabbit pulmonary artery smooth muscle. (**a**) Isometric tension recording showing the effects of 30 μ*M* cyclopiazonic acid (CPA) on a pulmonary arterial ring preincubated with 10 μ*M* nifedipine to inhibit L-type Ca^{2+} channels and the effect of the BK_{Ca} channel agonist NS-1619 in the continued presence of CPA and nifedipine. Thick bars above trace indicate drug applications. All solutions contained 1.8 m*M* Ca^{2+}. As indicated to the left of the trace, a 0.5-g resting tension was applied to the ring. Notice the transient and sustained contractions elicited by CPA and the enhancement of the CPA-induced sustained contraction by the hyperpolarization mediated by NS-1619. (**b**) Similar experiment to that shown in **a** except that store depletion was induced by 1 μ*M* thapsigargin (TG). (**c**) Plot of the time course of changes of normalized Fluo-4 fluorescence (F/F_0) in a freshly isolated pulmonary artery myocyte. The myocyte was preincubated for at least 10 min in Ca^{2+}-free solution prior to the beginning of the trace. As indicated, 30 μ*M* CPA evoked an initial Ca^{2+} transient consistent with Ca^{2+} leaking out of the sarcoplasmic reticulum due to blocking of Ca^{2+} reuptake. Readmitting extracellular Ca^{2+} ($[Ca]_o$ = 1.8 m*M*) in the continued presence of CPA and nifedipine led to the development of a robust Ca^{2+} transient consistent with SOCE

PSS (in m*M*): NaCl (120), KCl (4.2), $NaHCO_3$ (25; pH 7.4 after equilibration with 95% O_2/5% CO_2 gas), KH_2PO_4 (1.2), $MgCl_2$ (1.2), glucose (11), taurine (25), adenosine (0.01), and $CaCl_2$ (0.01 or 0.05). In the Fluo-4 experiments described in

Fig. 3.1c, single myocytes were superfused at room temperature with modified PSS composed of the following (in m*M*): NaCl (130), $NaHCO_3$ (10), KCl (4.2), KH_2PO_4 (1.2), $MgCl_2$ (0.5), $CaCl_2$ (0 or 1.8), glucose (5.5), and HEPES–NaOH (10; pH 7.35). The K^+-free bathing solution used in all patch clamp experiments had the following composition (in m*M*): NaCl (126), HEPES–NaOH (10; pH 7.35), tetraethyl-ammonium chloride (TEA) (8.4), glucose (20), $MgCl_2$ (1.2), and $CaCl_2$ (1.8). The pipet solution used in all perforated patch experiments had the following composition (in m*M*): Cs_2SO_4 (75), CsCl (55), HEPES–CsOH (10; pH 7.2), and $MgCl_2$ (5). Patch perforation was facilitated using the pore-forming antibiotic nystatin (400 mg/mL working concentration from a dimethyl sulfoxide (DMSO) stock solution of 60 mg/mL). For the dual patch clamp and fluorescence experiments (Fig. 3.4b), the pipet solution had the following composition (in m*M*): TEA (20), CsCl (106), 4-(2-hydroxyethyl)-1-piperazineethanesulfonic acid (HEPES)–CsOH (10; pH 7.2), ethylene glycol tetraacetic acid (EGTA) (1), adenosine triphosphate (ATP).Mg (3), guanosine triphosphate (GTP).diNa (0.2), and K_5-Fluo-5F (0.2). All enzymes, analytical-grade reagents, nifedipine, NS-1619, and niflumic acid (NFA) were purchased from Sigma-Aldrich. CPA and TG were purchased from Calbiochem; Fluo-4 AM and the pentapotassium salt of Fluo-5F were purchased from Molecular Probes. NFA, nifedipine, Fluo-4, CPA, TG, and NS-1619 were initially prepared as a stock solution in DMSO, and an appropriate aliquot was added to the external solution to reach the final desired concentration. The maximal concentration of DMSO never exceeded 0.1%, a concentration that had no effect on all parameters measured.

2.6 Reverse-Transcriptase Polymerase Chain Reaction Experiments

Total RNA was isolated from homogenates of whole rabbit PA, rabbit brain, and mouse brain using PureZol (Bio-Rad). Prior to preparing complementary DNA (cDNA), the RNA was treated with DNase I (Invitrogen) to prevent genomic DNA contamination. The cDNA was prepared using oligodeoxy thymidylic acid (oligo-dT) and dNTP (deoxynucleotide triphosphate) mixtures with Superscript II, with a negative reverse-transcriptase (RT) control prepared for each tissue sample (Invitrogen).

Rabbit sequences were available for TRPC1, 2, and 5, and primers were designed accordingly. For all the other genes (TRPC3, 4, 6, and 7; Orai1–3; STIM1 and 2; and TMEM16 A and B), no rabbit sequences were available, so degenerate polymerase chain reaction (PCR) primers designed against an alignment of a combination of the sequences available for mouse, rat, dog, cow, chimp, monkey, and human were generated. All primers were synthesized by Operon Biotechnologies. Amplification of the cDNA was performed using Gotaq (Promega), which had an amplification profile of an initial step to 95°C for 2 min to activate the Amplitaq polymerase, followed by 36 cycles of denaturation at 95°C for 30 s, annealing at T_a (°C) for 30 s, extension at 72°C for 30 s, followed by a final extension step of 72°C for 5 min, where T_a is the optimal annealing temperature for each primer pair

(range 60–63°C). The amplified products (10 μL) were separated by electrophoresis on a 2% agarose/Tris (tris (hydroxy-methyl) amino-methane), acetic acid, ethylenediaminetetraacetic acid (EDTA) gel, and the DNA bands were visualized by ethidium bromide staining. Both a negative RT control (described in the first paragraph of this section) and a nontemplate control for the master mix of reagents made for each primer pair were also run on the gels to ensure that no contamination was present. Once DNA bands were observed at the expected size, the remainder of the PCR samples were sent for sequencing, and the sequences that were obtained were blasted against the NCBI (National Center for Biotechnology Information) database to confirm the identity of the products. From this, nested primers were designed for those sequences determined through the use of degenerate primers, and the PCR reaction was rerun as described.

2.7 Statistical Analysis

All data were pooled from *n* cells taken from at least two different animals. All data were first amalgamated in Excel and means exported to Origin 7.5 software for plotting and curve fitting. All graphs, contractility, fluorescence, and current traces were exported to CorelDraw 12 for final processing of the figures. Origin 7.5 software was also used to determine the statistical significance between two groups using a paired Student *t* test. We considered $P < 0.05$ as statistically significant.

3 Results

3.1 Demonstration of Store-Operated Ca^{2+} Entry

We first determined whether SOCE could be detected in intact rabbit PAs exposed to blockers of the SERCA pump to deplete the SR Ca^{2+} stores. Figure 3.1a shows two typical experiments demonstrating that store depletion can elicit a contraction, and that altering membrane potential pharmacologically can modulate the contractile response. In these experiments, endothelium-denuded arteries were exposed to a physiological Ca^{2+} concentration in the bathing solution (1.8 m*M*) and to 10 μ*M* nifedipine to block Ca^{2+} entry through voltage-gated L-type Ca^{2+} channels. In panel A, exposure of the preparation to 30 μ*M* CPA, a specific and reversible blocker of SERCA, induced a rapid transient increase in force, which stabilized to an elevated and sustained level of contraction after about 8 min. Exposure of the preparation to an activator of large conductance Ca^{2+}-activated K^+ channels (BK_{Ca}), NS-1619[30] in the continued presence of CPA and nifedipine more than doubled the magnitude of the contraction. In 15 rings from five animals, the initial transient and sustained contractions evoked by CPA were 53 ± 17 mg and 68 ± 36 mg, respectively;

NS-1619 enhanced the CPA-induced contraction in 12 of 15 rings by 20 ± 4 mg. In separate experiments, preincubating arterial rings to nominally Ca^{2+}-free solution in the presence of nifedipine led to the disappearance of the initial transient contraction evoked by 30 μ*M* CPA. However, readmitting Ca^{2+} in the bathing medium consistently produced a sustained contraction of similar magnitude to the ones measured in the experiments described in panel a (data not shown). One possible explanation for such a difference is that Ca^{2+} omission combined with nifedipine may have already induced depletion of the stores prior to exposure to CPA. As shown in panel B, although the response was typically slower in onset, similar results were obtained with the other SERCA inhibitor TG. In six rings from two animals, 1 μ*M* TG induced transient and sustained contractions of 130 ± 37 mg and 175 ± 35 mg, respectively. In three of the six rings onto which NS-1619 was tested, the BK_{Ca} channel activator elicited a potent additional contraction of 180 ± 20 mg.

We next tested whether SOCE can be observed in freshly isolated myocytes, which will be used in subsequent patch clamp experiments. Figure 3.1b illustrates the result of one of five typical experiments in which free intracellular Ca^{2+} concentration was measured with the fluorescent Ca^{2+} indicator Fluo-4. The cell was preincubated for more than 5 min in a Ca^{2+}-free solution containing 10 μ*M* nifedipine before the application of CPA. Application of CPA caused a transient increase in fluorescence (~ twofold), which slowly returned to baseline. Reintroducing Ca^{2+} in the presence of CPA led to a more than sixfold increase in fluorescence, which is consistent with SOCE. Taken together, the contraction and fluorescence data demonstrate convincingly the existence of SOCE in rabbit PAs. The initial transient response to CPA or TG was consistent Ca^{2+} leakage in the cytoplasm following inhibition of Ca^{2+} reuptake in the SR, whereas the sustained response was the hallmark of SOCE. Further support to the latter comes from the demonstration of a contraction associated with hyperpolarization mediated by BK_{Ca} channels by NS-1619, which increases the driving force for Ca^{2+} entry.

3.2 SOCE Activates Ca^{2+}-Activated Cl^- Conductance

The possible activation of Cl_{Ca} by SOCE was investigated by using the perforated variant of the patch clamp technique. In these experiments, K^+ was substituted with Cs^+ in the pipet solution, and a K^+-free extracellular solution containing TEA was used to inhibit K^+ channels. Figure 3.2a shows ionic currents (top traces) evoked by the voltage clamp protocol shown at bottom. From an HP of –70 mV, a 250-ms step

Fig. 3.2 (continued) for the nonselective cation current triggered by store depletion. (**d**) Graph showing *I–V*s for peak current measured during step 2 (see **b**) as a function of voltage during step 1. Both sets of data were fitted to a single exponential function. Although both followed a similar trend, the current recorded in the presence of TG was greatly enhanced by preconditioning hyperpolarizing steps

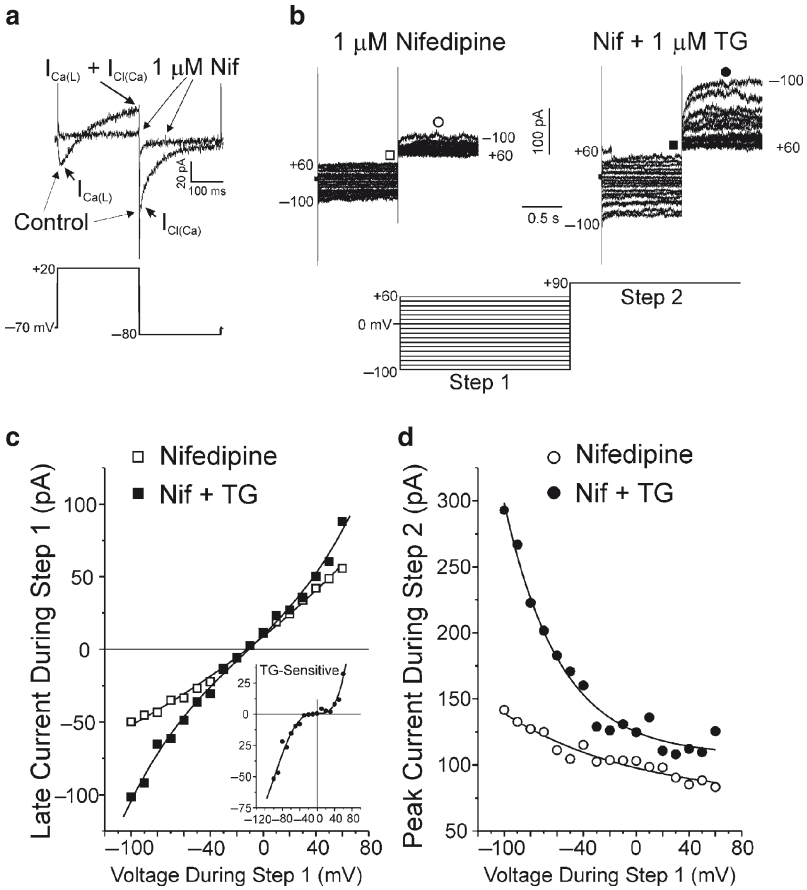

Fig. 3.2 Typical experiment demonstrating an interaction between a membrane current induced by store depletion and Ca^{2+}-activated Cl^- current in a rabbit pulmonary artery myocyte. All traces and graphs shown in **a**–**d** were derived from the same cell. (**a**) Superimposed membrane currents (*top*) elicited by the voltage clamp protocol shown at the *bottom,* which consisted of a 250-ms step to +20 mV from a holding potential of –70 mV, followed by a 250-ms return step to -80 mV. As indicated, the "Control" trace consists of an initial fast transient inward L-type Ca^{2+} current [$I_{Ca(L)}$] that reverses during inactivation to become an outward current composed of remaining $I_{Ca(L)}$ and Ca^{2+}-activated Cl^- current [$I_{Cl(Ca)}$]. The slow tail current is predominantly composed of $I_{Cl(Ca)}$ since deactivation of $I_{Ca(L)}$ is on the order of a few milliseconds. A 5-min application to 1 μ*M* nifedipine (Nif) abolished both components. (**b**) Two families of membrane currents recorded in the presence of 1 μ*M* nifedipine, before (*left*) and after (*right*) exposure to 1 μ*M* thapsigargin (TG) to deplete the stores. Each set of traces was generated by the double-pulse protocol shown below. The two steps were 1 s in duration. Notice that TG enhanced the magnitude of the time-independent current during step 1 and led to the appearance of a time-dependent Ca^{2+}-activated Cl^- current during step 2 (+90 mV) that grew with membrane hyperpolarization during the previous step. Symbols above traces correspond to where measurements were made and correspondingly plotted in **c** and **d**. (**c**) *I–V* relationships for the current measured at the end of step 1 (see **b**) in the absence (*open squares*) or presence (*filled squares*) of 1 μ*M* TG. Both *I–V*s reversed at –11 mV. *Inset:* Plot of the TG-sensitive *I–V* relationship obtained by subtraction of the data in the main graph. The *line* passing through the data points is a fourth-order polynomial fit. Notice the N-shaped relationship typical

to +20 mV elicited a rapid transient inward Ca^{2+} current that became outward after about 100 ms. Repolarization to −80 mV resulted in the appearance of a slow deactivating tail current, which reflects time-dependent closure of the outward current that developed during the preceding step. Figure 3.2a also shows that all time-dependent currents were abolished following the application of 1 μ*M* nifedipine. This experiment demonstrated the classical behavior in this and many other types of vascular smooth muscle cells (VSMCs) where Ca^{2+} influx associated with inward L-type current activates a slowly developing outward Ca^{2+}-activated Cl^- current, $I_{Cl(Ca)}$, during the step and inward $I_{Cl(Ca)}$ tail current following repolarization caused by Ca^{2+} removal and voltage-dependent deactivation. Traces shown on the left in Figure 3.2b were from the same cell as Figure 3.2a and were generated with the double-pulse protocol displayed below the traces. The same protocol was applied in the same cell after a 5-min exposure to 1 μ*M* TG in the presence of nifedipine (right traces) to induce SOCE. The closed and open symbols indicate where measurements were made to construct the corresponding current–voltage relationships (*I–V*) shown in Figure 3.2c and d. TG activated an instantaneous time-independent current during the first step, but more interestingly, it also triggered the appearance of a time-dependent outward current that is consistent with $I_{Cl(Ca)}$ in this preparation. Figure 3.2c shows the *I–V*s for the current obtained before (open squares) and after TG (filled squares). Both *I–V*s reversed at –11 mV, supporting the idea that the basal conductance under these conditions is nonselective. The inset displays the TG-sensitive *I–V* calculated by subtraction. The TG-activated conductance displayed a typical "N"-shaped *I–V*, showing signs of inward and outward rectification as reported in many other studies examining the properties of store depletion-activated ionic currents in VSMCs. Figure 3.2d shows two *I–V*s generated by plotting peak outward current during step 2 (+90 mV) as a function of voltage during step 1. The outward current declined exponentially in the presence of nifedipine alone from –100 to +60 mV, a process that was greatly accentuated by depleting the stores with TG.

Figure 3.3 shows a plot of the time course of changes of normalized peak outward current during step 2 for a typical experi ment carried out with CPA. Measurements from selected traces at the top labeled *a*, *b,* and *c* are correspondingly indicated on the plot below. A hint of time-dependent outward and inward tail currents were apparent in the presence of nifedipine alone (trace *a*). Application of CPA caused an initial transient increase in outward current followed by a delayed robust enhancement of the current. Such behaviors remarkably resemble those of SOCE described in Fig. 3.1. The enhancement of current was so great in this particular cell that the fully stimulated outward current (trace *b*) was time independent, and only a slowly deactivating tail current could be detected following repolarization. In this and all other similar experiments with CPA, the voltage dependence of the outward current exhibited a similar profile to that seen with TG (Fig. 3.2d), that is, a steep decline associated with membrane depolarization. NFA (100 μ*M*) potently inhibited the CPA-induced current to a level that was higher than that recorded in the absence of CPA and abolished the tail current (trace *c*). Even though the inward current during the step to –70 mV was also inhibited by NFA, we believe

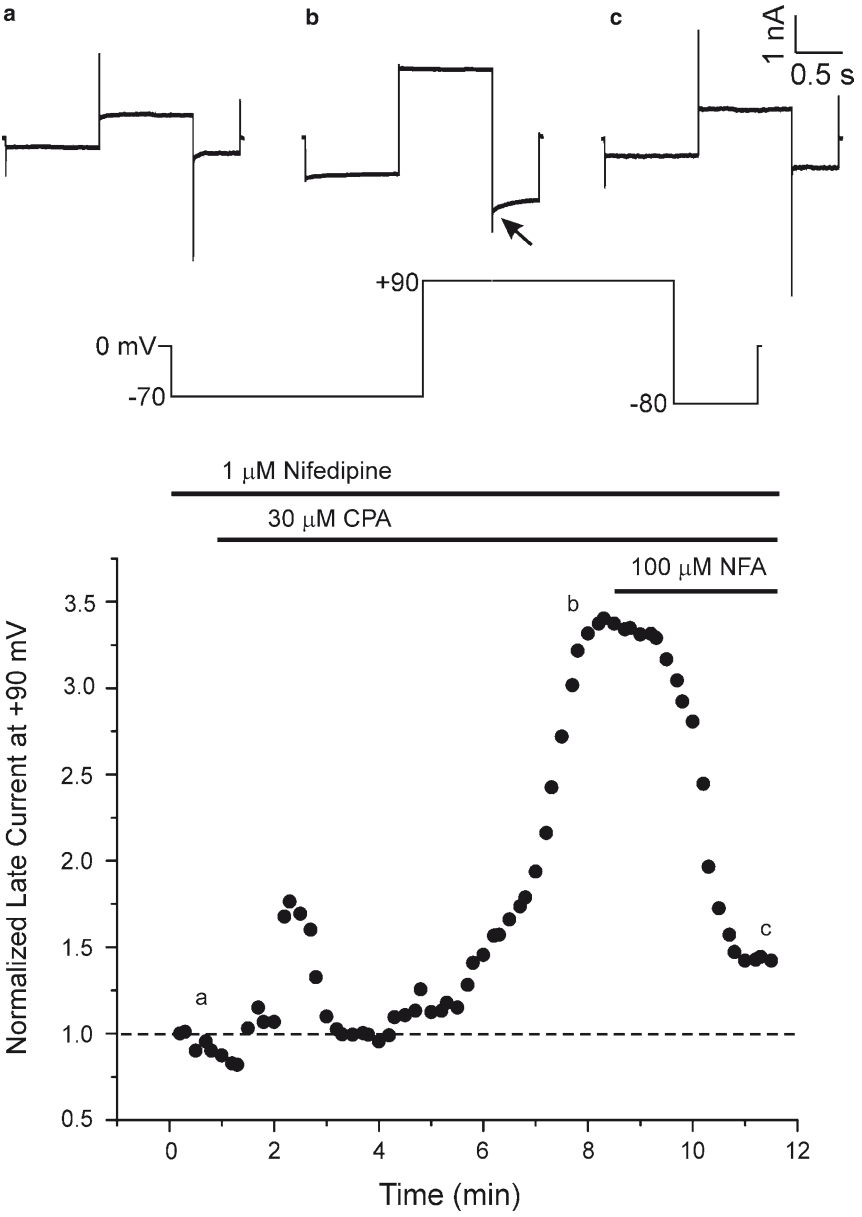

Fig. 3.3 The Ca^{2+}-activated Cl^- channel blocker niflumic acid (NFA) blocks a large component of membrane current activated by store depletion. Sample experiment from a rabbit pulmonary artery smooth muscle cell showing the effects of NFA on membrane currents evoked by the voltage clamp protocol shown below the traces. The three traces at the *top* were recorded in the presence of 1 μ*M* nifedipine alone (trace *a*) after full stimulation following exposure to 30 μ*M* cyclopiazonic acid (CPA; trace *b*) and following steady-state block by 100 μ*M* NFA (trace *c*). The *arrow* pointing at trace *b* indicates the appearance of a slow deactivating Ca^{2+}-activated Cl^- tail current. Measurements of current amplitude at the end of the step to +90 mV from these three traces were normalized to that recorded in the presence of nifedipine alone and are labeled in the graph below which shows the full time course of this experiment

that this reflected inhibition of $I_{Cl(Ca)}$ due to the very large basal activation of this current at the HP in this cell (0 mV). Indeed, significant deactivation of the current was evident at –70 mV in this cell (trace *b*). Analysis of the effects of NFA on the CPA-induced current at negative potentials revealed no significant differences between CPA and CPA plus NFA (e.g., at –50 mV, CPA 9.2 ± 3.0 pA/pF; CPA + NFA 8.8 ± 2.2 pA/pF; $P > 0.05$). These results suggest that NFA blocked $I_{Cl(Ca)}$ but not the SOCE-induced nonselective cation current. Finally, SKF-96365 (50 μ*M*), a widely used inhibitor of nonselective cation channels, suppressed the CPA-mediated time-independent current during the initial step (–100 to +60 mV), as well as time-dependent $I_{Cl(Ca)}$ during the second step to +90 mV (data not shown). In summary, our data provide evidence for a SKF-96365-sensitive SOCE pathway that allows for enhanced Ca^{2+} entry at negative potentials, which then serves as a trigger for activation of $I_{Cl(Ca)}$.

3.3 Voltage Dependence of SOCE and Impact on $I_{Cl(Ca)}$

We next sought to gain a better understanding of the properties of the source of Ca^{2+} entry activated by store depletion. In our initial voltage clamp experiments, we often observed that outward $I_{Cl(Ca)}$ reached a peak after a few hundred milliseconds and then slowly declined toward the end of the step. We hypothesized that activation and deactivation during the second step to +90 mV might be attributed to a complex pattern of voltage-dependent activation following the onset of the step and slow Ca^{2+} removal due to a decreased inwardly directed driving force for Ca^{2+} at positive potentials. This is better illustrated in the experiment shown in Fig. 3.4a. The voltage clamp protocol consisted of an initial 2-s step to –100 mV to increase Ca^{2+} entry following the application of CPA, followed by a 5-s step to +130 mV at which Ca^{2+} entry would be negligible. This panel clearly shows that after activation and stabilization for a few seconds, the current began to decrease progressively during the remainder of the step, in contrast with the maintenance of this current when intracellular Ca^{2+} is clamped with strong Ca^{2+} buffering with EGTA or 1,2-bis(o-aminophenoxy)ethane-N,N,N′N,N′-tetraacetic acid (BAPTA). To test this hypothesis more directly, we performed dual whole-cell voltage clamp experiments in myocytes dialyzed with the Ca^{2+} indicator Fluo-5 to monitor free $[Ca^{2+}]_i$ simultaneously. Figure 3.4b shows the results of one of three similar experiments carried out in the presence of nifedipine and CPA. While a step to +60 mV had no effect on the Fluo-5F signal and current, hyperpolarizing steps ranging from –60 to –100 mV led to voltage-dependent increases in $[Ca^{2+}]_i$ that were accompanied by time-dependent increases in inward current, most likely $I_{Cl(Ca)}$. Stepping to +90 mV caused an immediate exponential decline in $[Ca^{2+}]_i$. Again, progressively more negative voltage steps evoked progressively larger outward $I_{Cl(Ca)}$, which eventually declined over the course of the step, albeit at a slower rate than the Fluo-5F signal. These experiments lend support to the notion that store depletion evokes a Ca^{2+} entry pathway that is steeply dependent on the transmembrane Ca^{2+} driving force and that can stimulate Cl_{Ca} channels.

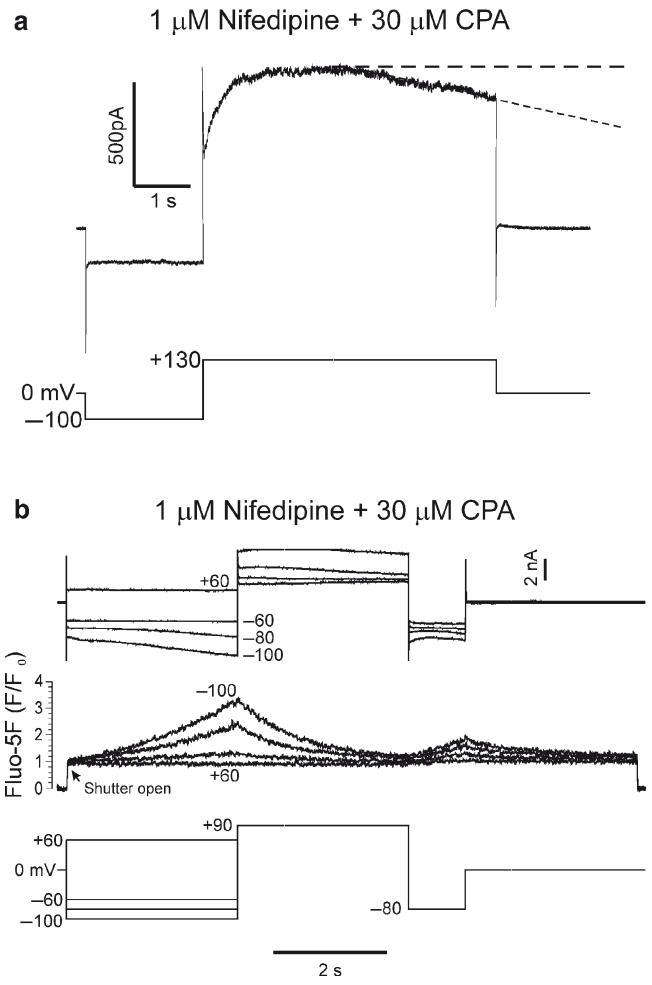

Fig. 3.4 Activation of Ca^{2+}-activated Cl^- conductance by store depletion depends on the transmembrane driving force for Ca^{2+}. (**a**) Typical membrane current (*top*) evoked by the protocol depicted below from pulmonary artery smooth muscle cells exposed to 1 μ*M* nifedipine and 30 μ*M* cyclopiazonic acid (CPA). The 2-s step to –100 mV was used to allow for Ca^{2+} entry through store-operated channels and was followed by a 5-s step to +130 mV (near the equilibrium potential for Ca^{2+}) to record Ca^{2+}-activated Cl^- current when Ca^{2+} entry is minimized. Notice the decline of time-dependent $I_{Cl(Ca)}$ (indicated by *dashed lines*) after activation and a temporary stabilization phase. (**b**) Dual-membrane current (*top traces*) and free intracellular Ca^{2+} concentration ($[Ca^{2+}]_i$; *middle traces*) recordings in a rabbit pulmonary artery myocyte dialyzed with 1 m*M* EGTA and 200 μ*M* Fluo-5 (K^+ salt form) and exposed to 1 μ*M* nifedipine and 30 μ*M* cyclopiazonic acid (CPA). The currents and Ca^{2+} transients were elicited by the voltage clamp protocol displayed below. Similar to Fig. 3.2, membrane current recorded during the second step to +90 mV increased with the magnitude of the preceding hyperpolarization and was consistent with the progressively larger Ca^{2+} transients detected. In contrast, stepping to +90 mV led to the immediate onset of an exponential decline in $[Ca^{2+}]_i$, which is consistent with store depletion triggering a Ca^{2+} entry pathway that is directly reliant on the Ca^{2+} driving force

3.4 Molecular Candidates for the Store-Operated Calcium Entry Pathway

Research has confirmed the importance of Orai, TRPC, and STIM as molecular entities involved in SOCE. We performed RT-PCR on cDNA made from isolated rabbit brain, rabbit PA, and mouse brain RNA, and nontemplate controls were run to control for primer contamination. Figure 3.5 shows the ethidium bromide-stained gel image for the PCR products. Gene expression for Orai1 was present in all three tissues, while Orai2 was confirmed only in the two brain samples (mouse and rabbit) and Orai3 only in the mouse brain (Fig. 3.5a). It is possible that the lack of evidence of Orai3 in the amplified rabbit cDNA samples is a facet of primer design rather than conclusive evidence that Orai3 is absent in the rabbit tissues. STIM1 and STIM2 gene expression was observed in mouse and rabbit brain and rabbit PA amplified cDNA samples (Fig. 3.5b). Various TRPC isoforms were detected in the amplified cDNA samples. In mouse brain, the TRPC1, 3, 4, 6, and 7 isoforms were detected. The primers for TRPC2 were not degenerate but designed against the rabbit sequence, suggesting that TRPC2 is not necessarily absent in this tissue, but that the primers were not specific enough to the species. With the exception of TRPC5 (not shown), all of the TRPC isoforms were detected in the rabbit brain (Fig. 3.5c). A similar pattern of expression was observed for the rabbit PA, although TRPC7 was undetectable (Fig. 3.5c). These data confirm the presence of many of the components necessary for a functional SOCE pathway to exist in the rabbit PA tissue.

3.5 Molecular Candidates for the Calcium-Activated Chloride Channel

We performed RT-PCR on cDNA made from isolated rabbit brain, rabbit PA, and mouse brain RNA, and nontemplate controls were run to control for primer contamination. Figure 3.5d shows evidence for detectable transcripts of both TMEM16A and TMEM16B in all three tissues, supporting a possible role for the TMEM16 family in the construction of the pore-forming subunit of Cl_{Ca} channels in the PA.

Fig. 3.5 (continued) rabbit sequences. (**b**) RT-PCR experiment carried out using degenerate primers for STIM1 and 2 (269 & 217 bp, respectively). Both STIM1 and 2 are present in the rabbit pulmonary artery, with additional unidentified bands observed. (**c**) RT-PCR experiment carried out using degenerate primers for TRPC3 (239 bp), 4 (242 bp), 6 (302 bp), and 7 (269 bp), and primers designed against available rabbit sequences for TRPC1 and 2 (479 and 235 bp, respectively). Most of the TRPC isoforms were present in the rabbit pulmonary artery (1–4 and 6); TRPC7 was absent. (**d**) RT-PCR experiment carried out using nested primers designed using rabbit sequences (obtained from previous experiments using degenerate primers) for TMEM16A (220 bp) and using degenerate primers for TMEM16B (377 bp). Both TMEM16A and TMEM16B are present in the rabbit pulmonary artery. Mouse brain and rabbit brain cDNA samples were consistently included in the experimental design as positive controls for the success of the degenerate primer design and their ability to detect sequences in rabbit tissues. All products obtained using degenerate primers were sequenced and blasted against the NCBI database to confirm identity

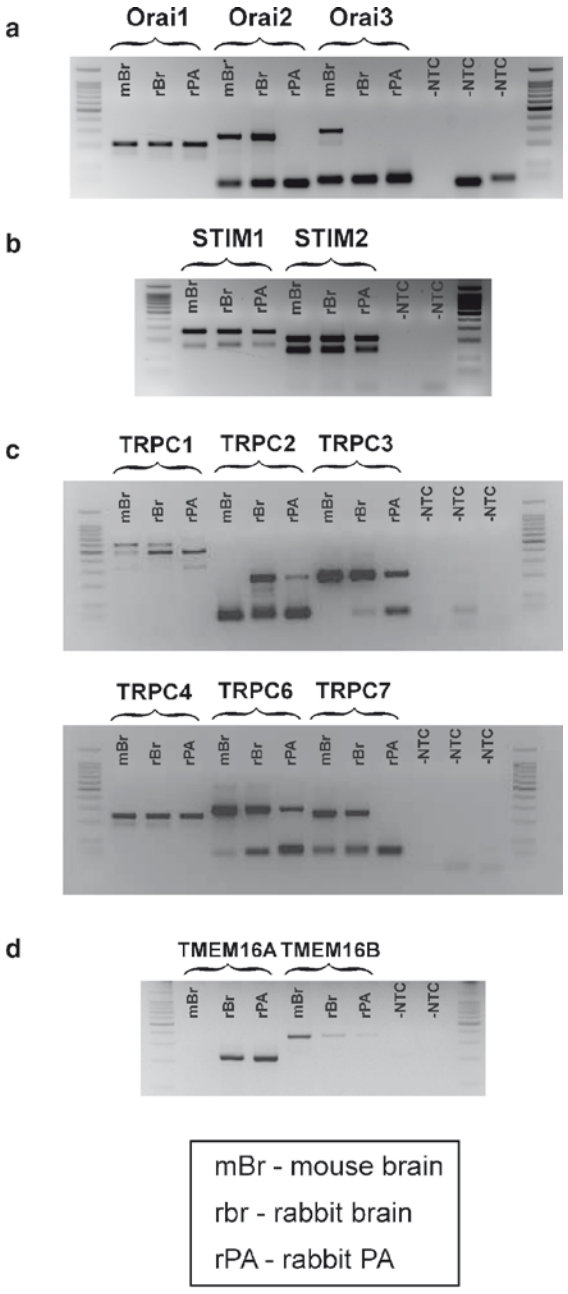

Fig. 3.5 Transcripts for some of the molecular candidates for store-operated calcium entry (SOCE) and the latest putative molecular candidate for the calcium-activated chloride channel (Cl_{Ca}) are expressed in rabbit pulmonary artery. (**a**) RT-PCR experiment carried out using degenerate primers for Orai1–3 (212, 238, and 313 bp, respectively). Only Orai1 appears to be present in the rabbit pulmonary artery, although the data for Orai3 remains inconclusive since these primer failed to detect a sequence in the rabbit brain, suggesting that they may be unsuccessful in detecting

4 Discussion

The primary objective of this investigation was to determine if store-operated Ca^{2+} entry is able to activate Ca^{2+}-activated Cl^- channels in PA myocytes, a major excitatory pathway in these vascular smooth muscle cells. We first showed that store depletion with the SR Ca^{2+}-ATPase (adenosine triphosphatase) inhibitor CPA or TG induced a sustained contraction of rabbit PAs that followed an initial transient contraction that was consistent with rapid leakage of Ca^{2+} out of the SR due to disruption of Ca^{2+} reuptake by TG or CPA. This contraction was independent of L-type Ca^{2+} channels since (1) nifedipine was present in all solutions and (2) cell hyperpolarization by activation of BK_{Ca} channels with NS-1619 led to enhancement of contraction instead of relaxation. Experiments carried out with freshly dispersed rabbit PA myocytes loaded with the Ca^{2+} indicator Fluo-4 demonstrated the persistence of an SOCE pathway following cell isolation, with an initial Ca^{2+} transient evoked by CPA in cells preincubated with nifedipine and the appearance of a large influx of Ca^{2+} following readmission of Ca^{2+} in the bathing medium. Store depletion with TG or CPA activated at least two distinct conductances in whole-cell path clamp experiments: (1) a time-independent SKF-96365-sensitive nonselective cation current reversing between –10 and 0 mV and (2) a time-dependent NFA-sensitive Cl_{Ca} current whose magnitude increased proportionately with preconditioning hyperpolarizing steps. Preliminary dual whole-cell patch clamp and Fluo-5F experiments to measure ionic currents and Ca^{2+} transients simultaneously showed that CPA-induced SOCE and activation of $I_{Cl(Ca)}$ were directly reliant on changes in the driving force for Ca^{2+}. Finally, our study provides strong evidence for the molecular expression of several key genetic components involved in SOCE and generation of Cl_{Ca} channels in rabbit PA smooth muscle.

4.1 Detection of SOCE-Induced Contraction in the Rabbit Pulmonary Arterial Vasculature

Store depletion induced by blocking Ca^{2+} reuptake into the SR, by releasing SR Ca^{2+} with caffeine, or following stimulation with G protein-coupled receptor agonists has been shown to induce Ca^{2+} influx or contraction in PAs[3,6,31] and smooth muscle cells from other vascular beds.[6,32] Our data in rabbit PA smooth muscle cells showed that exposure to a specific inhibitor of SERCA in Ca^{2+}-free medium elicits a Ca^{2+} transient that is manifest of Ca^{2+} leaking out of the SR when Ca^{2+} reuptake is impaired. Readmission of Ca^{2+} consistently led to a large insensitive elevation of intracellular free Ca^{2+} that is consistent with SOCE. As observed by others,[3,4] the Ca^{2+} signal was not sustained but partially declined to a stable elevated level that has been attributed to fast and slow Ca^{2+}-dependent inactivation modes of the store-operated channels.[33,34] In the presence of extracellular Ca^{2+}, the initial store depletion-induced Ca^{2+} transient and SOCE elicited corresponding contractions, indicating that SOCE is capable of generating PA tone in this species. Besides

insensitivity to block by the dihydropyridine nifedipine, which reportedly does not interfere with SOCE,[3] the store depletion-induced contraction was enhanced by NS-1619, a BK_{Ca} channel activator known to produce membrane hyperpolarization.[35] Such a behavior is anticipated for a Ca^{2+} entry pathway relying primarily on the electrochemical gradient for Ca^{2+}. This contrasts with the observation that NS-1619 causes relaxation of blood vessels contracted by agonists involving membrane depolarization and activation of voltage-gated Ca^{2+} channels, although there is evidence for direct block of Ca^{2+} channels.[35]

4.2 SOCE Activates Ca^{2+}-Activated Cl^- Current

The most interesting observation of the present study was the demonstration of a unique interaction between SOCE and Cl_{Ca} channels in our single-cell preparation. This was complicated by the scarcity and relatively poor specificity of pharmacological tools that rendered current separation difficult. We first took advantage of the voltage clamp technique to distinguish the store-operated cation current (I_{SOC}) and $I_{Cl(Ca)}$ on the basis that the former is known to generate sustained time-independent currents[3,9], whereas the latter displays pronounced outward rectification due to voltage- and time-dependent gating properties[20,29,36] and store depletion induced by TG or CPA elicited time-independent current that reversed between –10 and 0 mV. This is in accord with a nonselective cation current that would display significant permeability to Cs^+, Na^+, and Ca^{2+}, the major cation charge carriers used in our patch clamp experiments. The steady-state current–voltage relationship for this current measured at the end of 1-s steps from an HP of 0 mV exhibited the typical N shape, a behavior similar to that observed by others.[9] All our protocols consisted of an initial step to a range of potentials to evoke I_{SOC} followed by a second step at +90 mV or higher. The rationale for this second step was to minimize SOCE due to a dramatically reduced driving force for Ca^{2+} and to take advantage of the outwardly rectifying properties of $I_{Cl(Ca)}$. Keeping this second step constant enabled us to gauge Ca^{2+} entry through I_{SOC} and to monitor its effect on the magnitude of time-dependent $I_{Cl(Ca)}$ and indirectly free intracellular Ca^{2+} concentration.

Our data showed that in the presence of CPA or TG, activation of $I_{Cl(Ca)}$ at +90 mV followed a similar trend to that observed with the Ca^{2+} indicator Fluo-4 in single cells or contraction in PA rings with the detection of an initial and delayed and more robust component of outward current. A substantial fraction of this time-dependent outward current was blocked by NFA, a commonly used inhibitor of Cl_{Ca} channels.[19,20] Time-dependent $I_{Cl(Ca)}$ at +90 mV was also progressively enhanced by preconditioning hyperpolarizing steps. Whereas the relatively uncontaminated I_{SOC} elicited during the first step was insensitive to NFA, time-dependent $I_{Cl(Ca)}$ at +90mV and its slow deactivating tail current after repolarization to -80 mV were potently inhibited by the fenamate. Both I_{SOC} and $I_{Cl(Ca)}$ were strongly inhibited by SKF-96365, a potent blocker of SOCE and I_{SOC}.[9] Although this observation supports a possible role for Ca^{2+} entry through I_{SOC} in eliciting $I_{Cl(Ca)}$, we cannot rule out the

possibility of a direct inhibitory effect of this blocker on Cl_{Ca} channels that should be tested on $I_{Cl(Ca)}$ recorded in isolation by clamping $[Ca^{2+}]_i$ to known fixed elevated levels.

To obtain more direct proof of SOCE induced by hyperpolarization and subsequent activation of $I_{Cl(Ca)}$, we measured Ca^{2+} transients simultaneously with membrane current in whole-cell voltage-clamped PA myocytes dialyzed with Fluo-5 and exposed to CPA and nifedipine. Consistent with this hypothesis, graded Ca^{2+} entry was elicited in response to hyperpolarizing steps and was mirrored by the progressively larger amplitude of $I_{Cl(Ca)}$ during a following step to +90 mV. In agreement with this idea, $[Ca^{2+}]_i$ declined exponentially at positive potentials, an observation in line with the marked reduction in driving force for Ca^{2+} at positive potentials. The magnitude of the Ca^{2+} transient and $I_{Cl(Ca)}$ thus appears to follow the changes in Ca^{2+} driving force imposed by membrane potential during the initial step. A report in airway smooth muscle[37] has suggested that Ca^{2+} entry via reverse-mode Na^+/Ca^{2+} exchange was the main source of Ca^{2+} responsible for the contraction induced by SOCE. In this paradigm, Na^+ entry through I_{SOC} would raise intracellular Na^+ levels, causing a negative shift in the reversal potential of the exchanger ($E_{NCX} = 3E_{Na} - 2E_{Ca}$ assuming a stochiometry of $3Na^+$:1 Ca^{2+}) favoring net Ca^{2+} entry. We purposely dialyzed the myocyte with a Na^+-free pipet solution to minimize this effect. However, it is still possible that enough Na^+ entry through I_{SOC} during a hyperpolarizing step accumulates in a restricted compartment, allowing for Ca^{2+} to be transported into the cell by the exchanger and stimulate $I_{Cl(Ca)}$. This important aspect of the pathway will require further investigation by examining whether external Na^+ removal has any effect on $[Ca^{2+}]_i$ and $I_{Cl(Ca)}$.

4.3 Nature of the Ca^{2+} Entry Pathway Stimulating Cl_{Ca} Channels

The membrane current activated by CPA or TG in our experiments is clearly a nonselective cation current, and preliminary experiments suggest, as other studies have implied in vascular smooth muscle cells,[3,9] that external Na^+ and internal Cs^+ are the main charge carriers in our recording conditions. Several members of the TRPC family (TRPC1, TRPC4, TRPC5, and in some studies TRPC6) of ion channels have originally been suggested to form the basis of I_{SOC} in many cell types.

Using an antibody targeting an extracellular epitope and used as a blocker, Xu and Beech[4] initially hypothesized TRPC1 to be a major component of this current in vascular smooth muscle. There are also suggestions, mainly from studies of overexpression in heterologous cell systems, that I_{SOC} may be formed from TRPC1 partnering with TRPC4 or TRPC5 in heteromultimeric complexes.[9,38] More recent reports have convincingly demonstrated that more than one molecular mechanism may be responsible for SOCE in smooth muscle. One study challenged the previously considered dogma that TRPC1 is "the" protein responsible for SOCE in smooth muscle. Dietrich et al.[39] showed that SOCE in aortic and cerebral vascular smooth muscle cells from $TRPC1^{-/-}$ was indistinguishable from wild type. At least one report provided evidence for TRPC6 playing a role in determining SOCE in

cultured rat PA smooth muscle cells[40] as well as in receptor-operated channel activity activated by α_1-adrenoceptor stimulation leading to production of the second messenger DAG,[41,42] and stimulation of protein kinase C[5] or stretch-activated nonselective cation channels.[43]

In addition to the Orais, two STIM isoforms (STIM1 and 2) have been reported in relation to SOCE. Current evidence suggests that STIM1 is located in the membrane of the ER and acts as a Ca^{2+} sensor for the ER Ca^{2+} stores,[44,45] interacting directly with Orai1 to initiate SOCE. Current thinking suggests that STIM2 interacts with STIM1 to inhibit STIM1-mediated activation of SOCE.[46]

These exciting discoveries have unraveled a new level of complexity in cellular signaling. Our molecular data provided evidence for the expression of transcripts encoding for TRPC1, 4, and 6; Orai1 and Orai2 but not Orai3; as well as STIM1 and STIM2, all of which have been suggested to play a role in SOCE. Although TRPC5 has been detected and suggested to participate in SOCE in pial arterioles,[47] we were unable to identify messenger RNA (mRNA) for this subunit in our preparation, and this may or may not be due to the rather incomplete rabbit genome. There is now convincing evidence that STIM1 is an integral part of the molecular architecture sensing ER Ca^{2+} levels and leading to activation of TRPC1,[15,17,48] and that Orai1 can form a ternary dynamic complex with STIM1 and TRPC1 following store depletion dictating SOCE.[16,49,50] STIM2 was initially suggested to antagonize the effects of STIM1 on SOCE.[46] More recent reports indicated that STIM2 may also serve as an ER Ca^{2+} sensor and stimulate SOCE, but its dynamic range and role in controlling ER and cytoplasmic Ca^{2+} levels appears to be different.[51,52] Clearly, a lot more work lies ahead to determine the distribution and function of these proteins in PA smooth muscle cells.

As shown in this and previous studies from our group, rabbit PA smooth muscle cells exhibit a large $I_{Cl(Ca)}$ that is activated by an elevation in internal Ca^{2+}, displays strong outward rectification due to voltage-dependent gating, and is downregulated by phosphorylation.[28,29,36] A search for the molecular candidate underlying this channel has highlighted a number of possibilities to date. Previous studies have suggested that Tweety, *CLCA,* or Bestrophins may be contenders; however, these candidates generally produce membrane currents that are for the most part dissimilar to that recorded from native Cl_{Ca} channels.[20,22] More recent evidence suggested that TMEM16A (Anoctamin; ANO1) and possibly TMEM16B (ANO2) are better molecular candidates for this channel.

Yang et al.[26] showed that currents measured in HEK293T cells in which ANO1 had been overexpressed displayed a small unitary conductance, were outwardly rectifying, and exhibited Ca^{2+} and voltage dependence. Furthermore, 4, 4′-diisothiocyanatostilbene-2, 2′-disulfonic acid (DIDS) and niflumic acid both inhibited these currents. This work was supported by that of Schroeder et al.,[25] who also demonstrated that overexpression of either TMEM16A or TMEM16B results in the generation of Cl_{Ca} currents.

We previously demonstrated the expression of several Bestrophins in the rabbit PA.[20] The present study further extended this analysis by showing that TMEM16A and B are also expressed at the mRNA level. It will be necessary to determine the exact role of these proteins in generating $I_{Cl(Ca)}$ and assess whether Bestrophins interact physically and functionally with TMEM16 proteins.

Many questions remain unanswered with respect to the Ca^{2+} entry pathways. Is Ca^{2+} entering the myocyte through the nonselective TRPC1 (and possibly others), the Ca^{2+}-selective Orai1 (CRACM1), or both? Are Ca^{2+}-activated Cl^- channels (TMEM16A or B? Bestrophins?) located in the vicinity of the SOCE pathways and triggered by a preferential subsarcolemmal compartment accessible to both? There is also evidence for STIM1-induced TRPC1 translocation into lipid rafts and caveolae during store depletion[15] and for an important role played by caveolin-1 in this process in vascular smooth muscle cells.[53]

5 Conclusion

This study shed some light on a new mechanism of interaction between two excitatory ionic mechanisms in smooth muscle. Our data confirm that a Ca^{2+} entry pathway consistent with store-operated Ca^{2+} entry signaling can activate Ca^{2+}-activated Cl^- channels in PA myocytes (Fig. 3.6). We hypothesize that this mecha-

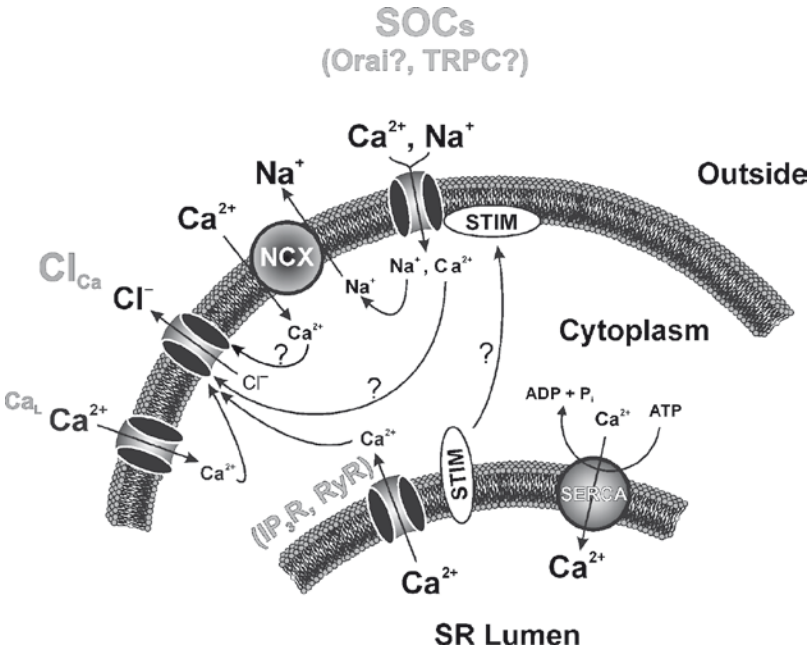

Fig. 3.6 Schematic diagram illustrating the different sources of Ca^{2+}, including those elicited by store depletion, that regulate Ca^{2+}-activated Cl^- channels in pulmonary artery smooth muscle cells. See text for explanations. Cl_{Ca} Ca^{2+}-activated Cl^- channels; Ca_L L-type Ca^{2+} channels; *SOCs* store-operated channels; Orai, STIM, and TRPC are the three candidate gene families proposed to support store-operated calcium entry in various cell types; *NCX* Na^+/Ca^{2+} exchanger; *SERCA* Ca^{2+}-ATPase in the sarcoplasmic reticulum (SR); IP_3R inositol trisphosphate receptor; *RyR* ryanodine receptor

nism may be important in the regulation of membrane potential, Ca^{2+} influx, and tone in these cells under physiological and pathophysiological conditions. Stimulation by Cl_{Ca} channels by SOCE may depolarize the cell toward E_{Cl} (~ –20 mV in smooth muscle) and thus reduce the transmembrane gradient for Ca^{2+}. Future studies should be undertaken to test the hypothesis that blocking Cl_{Ca} channels due to the ensuing hyperpolarization enhances SOCE.

Acknowledgments We wish to thank Janice Tinney and Marissa Huebner for their technical support in isolating PA smooth muscle cells and preparing solutions. This study was supported by a grant to N.L. from the National Institutes of Health (grant 5 RO1 HL 075477) and a grant to I.A.G. from the British Heart Foundation (PG/05/038). Publication was also made possible by grants to N.L. (NCRR 5 P20 RR15581) from the National Center for Research Resources, a component of the National Institutes of Health (NIH) supporting two Centers of Biomedical Research Excellence (COBRE) at the University of Nevada School of Medicine, Reno, Nevada. The contents of the chapter are solely the responsibility of the authors and do not necessarily represent the official views of NCRR or NIH.

References

1. Bygrave FL, Roberts HR (1995) Regulation of cellular calcium through signaling cross-talk involves an intricate interplay between the actions of receptors, G-proteins, and second messengers. FASEB J 9:1297–1303
2. Putney JW, Broad LM, Braun FJ, Lievremont JP, Bird GSJ (2001) Mechanisms of capacitative calcium entry. J Cell Sci 114:2223–2229
3. Ng LC, Gurney AM (2001) Store-operated channels mediate Ca^{2+} influx and contraction in rat pulmonary artery. Circ Res 89:923–929
4. Xu SZ, Beech DJ (2001) TrpC1 is a membrane-spanning subunit of store-operated Ca^{2+} channels in native vascular smooth muscle cells. Circ Res 88:84–87
5. Albert AP, Large WA (2002) A Ca^{2+}-permeable non-selective cation channel activated by depletion of internal Ca^{2+} stores in single rabbit portal vein myocytes. J Physiol 538:717–728
6. Wilson SM, Mason HS, Smith GD et al (2002) Comparative capacitative calcium entry mechanisms in canine pulmonary and renal arterial smooth muscle cells. J Physiol 543:917–931
7. Prakriya M, Lewis RS (2003) CRAC channels: activation, permeation, and the search for a molecular identity. Cell Calcium 33:311–321
8. Albert AP, Large WA (2003) Store-operated Ca^{2+}-permeable non-selective cation channels in smooth muscle cells. Cell Calcium 33:345–356
9. Beech DJ, Muraki K, Flemming R (2004) Non-selective cationic channels of smooth muscle and the mammalian homologues of Drosophila TRP. J Physiol 559:685–706
10. Lewis RS (2007) The molecular choreography of a store-operated calcium channel. Nature 446:284–287
11. Feske S, Gwack Y, Prakriya M et al (2006) A mutation in Orai1 causes immune deficiency by abrogating CRAC channel function. Nature 441:179–185
12. Prakriya M, Feske S, Gwack Y, Srikanth S, Rao A, Hogan PG (2006) Orai1 is an essential pore subunit of the CRAC channel. Nature 443:230–233
13. Mercer JC, DeHaven WI, Smyth JT et al (2006) Large store-operated calcium selective currents due to co-expression of Orai1 or Orai2 with the intracellular calcium sensor, Stim1. J Biol Chem 281:24979–24990
14. Luik RM, Wu MM, Buchanan J, Lewis RS (2006) The elementary unit of store-operated Ca^{2+} entry: local activation of CRAC channels by STIM1 at ER-plasma membrane junctions. J Cell Biol 174:815–825

15. Alicia S, Angelica Z, Carlos S, Alfonso S, Vaca L (2008) STIM1 converts TRPC1 from a receptor-operated to a store-operated channel: moving TRPC1 in and out of lipid rafts. Cell Calcium 44:479–491
16. Ong HL, Cheng KT, Liu X et al (2007) Dynamic assembly of TRPC1-STIM1-Orai1 ternary complex is involved in store-operated calcium influx. Evidence for similarities in store-operated and calcium release-activated calcium channel components. J Biol Chem 282:9105–9116
17. Li J, Sukumar P, Milligan CJ et al (2008) Interactions, functions, and independence of plasma membrane STIM1 and TRPC1 in vascular smooth muscle cells. Circ Res 103:e97–e104
18. Liao Y, Erxleben C, Abramowitz J et al (2008) Functional interactions among Orai1, TRPCs, and STIM1 suggest a STIM-regulated heteromeric Orai/TRPC model for SOCE/Icrac channels. Proc Natl Acad Sci U S A 105:2895–2900
19. Large WA, Wang Q (1996) Characteristics and physiological role of the Ca^{2+}-activated Cl^- conductance in smooth muscle. Am J Physiol 271:C435–C454
20. Leblanc N, Ledoux J, Saleh S et al (2005) Regulation of calcium-activated chloride channels in smooth muscle cells: a complex picture is emerging. Can J Physiol Pharmacol 83:541–556
21. Hartzell C, Putzier I, Arreola J (2005) Calcium-activated chloride channels. Annu Rev Physiol 67:719–758
22. Hartzell HC, Qu Z, Yu K, Xiao Q, Chien LT (2008) Molecular physiology of bestrophins: multifunctional membrane proteins linked to best disease and other retinopathies. Physiol Rev 88:639–672
23. Hartzell HC, Yu K, Xiao Q, Chien LT, Qu Z (2009) Anoctamin/TMEM16 family members are Ca^{2+}-activated Cl– channels. J Physiol 587(Pt 10):2127–2139
24. Caputo A, Caci E, Ferrera L et al (2008) TMEM16A, a membrane protein associated with calcium-dependent chloride channel activity. Science 322:590–594
25. Schroeder BC, Cheng T, Jan YN, Jan LY (2008) Expression cloning of TMEM16A as a calcium-activated chloride channel subunit. Cell 134:1019–1029
26. Yang YD, Cho H, Koo JY et al (2008) TMEM16A confers receptor-activated calcium-dependent chloride conductance. Nature 455:1210–1215
27. Lin MJ, Leung GPH, Zhang WM et al (2004) Chronic hypoxia-induced upregulation of store-operated and receptor-operated Ca^{2+} channels in pulmonary arterial smooth muscle cells — A novel mechanism of hypoxic pulmonary hypertension. Circ Res 95:496–505
28. Greenwood IA, Ledoux J, Sanguinetti A, Perrino BA, Leblanc N (2004) Calcineurin Aα but not Aβ augments $I_{Cl(Ca)}$ in rabbit pulmonary artery smooth muscle cells. J Biol Chem 279:38830–38837
29. Angermann JE, Sanguinetti AR, Kenyon JL, Leblanc N, Greenwood IA (2006) Mechanism of the inhibition of Ca^{2+}-activated Cl^- currents by phosphorylation in pulmonary arterial smooth muscle cells. J Gen Physiol 128:73–87
30. Edwards G, Niederstehollenberg A, Schneider J, Noack T, Weston AH (1994) Ion channel modulation by NS 1619, the putative BK_{Ca} channel opener, in vascular smooth muscle. Br J Pharmacol 113:1538–1547
31. McDaniel SS, Platoshyn O, Wang J et al (2001) Capacitative Ca^{2+} entry in agonist-induced pulmonary vasoconstriction. Am J Physiol Lung Cell Mol Physiol 280:L870–L880
32. Leung FP, Yung LM, Yao X, Laher I, Huang Y (2008) Store-operated calcium entry in vascular smooth muscle. Br J Pharmacol 153:846–857
33. Zweifach A, Lewis RS (1995) Slow calcium-dependent inactivation of depletion-activated calcium current. Store-dependent and -independent mechanisms. J Biol Chem 270:14445–14451
34. Zweifach A, Lewis RS (1995) Rapid inactivation of depletion-activated calcium current (i_{CRAC}) due to local calcium feedback. J Gen Physiol 105:209–226
35. Holland M, Langton PD, Standen NB, Boyle JP (1996) Effects of the BK_{Ca} channel activator, NS1619, on rat cerebral artery smooth muscle. Br J Pharmacol 117:119–129
36. Greenwood IA, Ledoux J, Leblanc N (2001) Differential regulation of Ca^{2+}-activated Cl^- currents in rabbit arterial and portal vein smooth muscle cells by Ca^{2+}-calmodulin-dependent kinase. J Physiol 534:395–408

37. Hirota S, Pertens E, Janssen LJ (2007) The reverse mode of the Na^+/Ca^{2+} exchanger provides a source of Ca^{2+} for store refilling following agonist-induced Ca^{2+} mobilization. Am J Physiol Lung Cell Mol Physiol 292:L438–L447
38. Vazquez G, Wedel BJ, Aziz O, Trebak M, Putney JW Jr (2004) The mammalian TRPC cation channels. Biochim Biophys Acta 1742:21–36
39. Dietrich A, Kalwa H, Storch U et al (2007) Pressure-induced and store-operated cation influx in vascular smooth muscle cells is independent of TRPC1. Pflugers Arch 455:465–477
40. Yu Y, Sweeney M, Zhang S et al (2003) PDGF stimulates pulmonary vascular smooth muscle cell proliferation by upregulating TRPC6 expression. Am J Physiol Cell Physiol 284:C316–C330
41. Inoue R, Okada T, Onoue H et al (2001) The transient receptor potential protein homologue TRP6 is the essential component of vascular α_1-adrenoceptor-activated Ca^{2+}-permeable cation channel. Circ Res 88:325–332
42. Jung S, Strotmann R, Schultz N, Plant TD (2002) TRPC6 is a candidate channel involved in receptor-stimulated cation currents in A7r5 smooth muscle cells. Am J Physiol Cell Physiol 282:C347–C359
43. Welsh DG, Morielli AD, Nelson MT, Brayden JE (2002) Transient receptor potential channels regulate myogenic tone of resistance arteries. Circ Res 90:248–250
44. Liou J, Kim ML, Heo WD et al (2005) STIM is a Ca^{2+} sensor essential for Ca^{2+}-store-depletion-triggered Ca^{2+} influx. Curr Biol 15:1235–1241
45. Zhang SL, Yu Y, Roos J et al (2005) STIM1 is a Ca^{2+} sensor that activates CRAC channels and migrates from the Ca^{2+} store to the plasma membrane. Nature 437:902–905
46. Soboloff J, Spassova MA, Hewavitharana T et al (2006) STIM2 is an inhibitor of STIM1-mediated store-operated Ca^{2+} entry. Curr Biol 16:1465–1470
47. Xu SZ, Boulay G, Flemming R, Beech DJ (2006) E3-targeted anti-TRPC5 antibody inhibits store-operated calcium entry in freshly isolated pial arterioles. Am J Physiol Heart Circ Physiol 291:H2653–H2659
48. Huang GN, Zeng W, Kim JY et al (2006) STIM1 carboxyl-terminus activates native SOC, I_{crac} and TRPC1 channels. Nat Cell Biol 8:1003–1010
49. Cheng KT, Liu X, Ong HL, Ambudkar IS (2008) Functional requirement for Orai1 in store-operated TRPC1-STIM1 channels. J Biol Chem 283:12935–12940
50. Jardin I, Lopez JJ, Salido GM, Rosado JA (2008) Orai1 mediates the interaction between STIM1 and hTRPC1 and regulates the mode of activation of hTRPC1-forming Ca^{2+} channels. J Biol Chem 283:25296–25304
51. Brandman O, Liou J, Park WS, Meyer T (2007) STIM2 is a feedback regulator that stabilizes basal cytosolic and endoplasmic reticulum Ca^{2+} levels. Cell 131:1327–1339
52. Stathopulos PB, Zheng L, Ikura M (2009) Stromal interaction molecule (STIM) 1 and STIM2 calcium sensing regions exhibit distinct unfolding and oligomerization kinetics. J Biol Chem 284:728–732
53. Ingueneau C, Huynh-Do U, Marcheix B et al (2008) TRPC1 is regulated by caveolin-1 and is involved in oxidized LDL-induced apoptosis of vascular smooth muscle cells. J Cell Mol Med Nov 14 [Epub ahead of print]